

# Inferring the Nuclear Equation of State Using Gravitational Waves from Binary Neutron Star Mergers †

Samantha A. Usman<sup>1</sup>

Advisors: Tjonnie Li<sup>2</sup>, Alan Weinstein<sup>2</sup>

<sup>1</sup> Department of Physics, Syracuse University, Syracuse, NY 13244, USA

<sup>2</sup> LIGO Laboratory, California Institute of Technology, Pasadena, CA 91125, USA

E-mail: [samantha.usman@ligo.org](mailto:samantha.usman@ligo.org)

**Abstract.** We study how the Laser Interferometer Gravitational-Wave Observatory (LIGO) can be used to learn more about the nuclear equation-of-state. The equation-of-state for nuclear matter describes how matter behaves at different densities. Since we cannot recreate such high densities on Earth, we turn to astrophysical sources to learn more about their structure. Gravitational waves from binary neutron star mergers can give us insight into the nature of matter at high densities. First, we describe the current state of research on the subject and the motivation behind this project. We then show how gravitational-wave detections from binary neutron-star systems are sensitive to variations in tidal deformabilities. This information about neutron stars' tidal deformability will constrain the nuclear equation-of-state. We describe the deformation and disruption with a single parameter that affects the gravitational waveform and estimate it using analysis pipeline which we describe here. This estimation will allow us to quantify the pipeline's precision as the number of gravitational-wave detections from binary neutron star systems grows. The deformability will give us new information about the nuclear equation-of-state and will rule out unlikely models. Finally, we compare the pipeline's performance on three possible nuclear equation-of-state models to learn how well the pipeline can differentiate between them.

## 1. Introduction

The nuclear equation-of-state (EOS) determines how the matter acts under different densities and pressures. While we understand how matter behaves at low densities, higher densities (like those found in neutron stars) are impossible to recreate on earth. The behavior of matter at these densities is of great interest since neutron stars are of similar density to atomic nuclei. For these reasons, we turn to gravitational waves to learn more about the nuclear EOS.

Gravitational waves are ripples in spacetime which cause the distance between freely falling test masses to vary. The Laser Interferometer Gravitational-Wave Observatory

(LIGO) aims to detect gravitational waves from astrophysical sources. A network of interferometric detectors has been constructed, including LIGO in the United States [1] and international detectors including VIRGO in Pisa [2], Italy and the Kamioka Gravitational Wave Detector (KAGRA) in Japan [3]. This international network allows scientists to verify that a detected gravitational wave has passed throughout Earth and was not simply a misidentification in a single detector.

In recent years, the LIGO detectors have undergone many modifications. These changes to the equipment will allow the detectors to reduce their background noise and reach a new level of sensitivity. This design sensitivity will be reached during the early runs of the newly renovated detectors, now called Advanced LIGO (aLIGO), allowing us to detect waves from further into the universe than ever before.

LIGO uses laser interferometry to detect the stretching and squeezing of spacetime caused by gravitational waves. Black holes and neutron stars orbiting in binaries are likely to be strong sources of gravitational waves for aLIGO [4]. By detecting waves from binary neutron stars (BNS), we can learn more about the physics of compact objects. For gravitational waves from a binary neutron star system at a distance  $r$  from the observer, the strain observable by the LIGO detectors can be approximated by

$$h \approx \frac{GT}{c^4 r}, \quad (1)$$

where  $T$  represents the kinetic energy from the quadrupole moment. The gravitational constant and the speed of light are denoted  $G$  and  $c$ , respectively. In a binary system, the kinetic energy goes with the square of the separation (denoted  $a$ ) and inversely with the square of the period of the orbit (denoted  $P$ )

$$T \approx M \left( \frac{\pi a}{P} \right)^2, \quad (2)$$

where  $M$  is the total mass of the binary. Radio observations of neutron stars in binaries suggest that the neutron stars have masses around  $1.35 M_\odot$  [5]. Kepler's third law relates the period to the separation of the bodies

$$P^2 = \frac{4\pi^2 a^3}{GM}. \quad (3)$$

Orbital frequency of a binary is half its gravitational-wave frequency.

We can do a simple qualitative argument to approximate the sensitivity necessary to detect gravitational waves from the systems. Thus to have a 200 Hz gravitational wave, a binary must have an orbital frequency of 100 Hz. Since seismic noise overwhelms lower frequencies and photon shot noise overwhelms higher frequencies, ground-based detectors like LIGO are most sensitive to frequencies between 100 and 500 Hz. Assuming a binary's gravitational wave is in the most sensitive range of LIGO, we can estimate its orbital frequency to be about 100 Hz. Approximating that the total mass in a BNS system is  $2.7 M_\odot$ , about  $5 \times 10^{30}$  kg, and the period to be about 1/100 seconds, we find that such a binary would have kinetic energy of about  $5 \times 10^{45}$  kg  $\times$  m<sup>2</sup>/s<sup>2</sup>. This means

that a binary 100 Mpc away would have a strain of about  $10^{-22}$ . In order to detect such small amplitudes, the detectors must be very sensitive to these small changes in length. After aLIGO reaches design sensitivity, we expect to detect between 0.4 and 400 gravitational wave signals from BNS per year. These signals correspond to a signal-to-noise ratio of at least 8, which is loud enough compared to the detectors' background noise to claim a detection [6].

In post-Newtonian theory, we can derive the gravitational waveform from the energy balance equation. This states that the energy loss is equal to the energy flux radiated in gravitational waves by

$$\frac{dE}{dt} = -\mathcal{F}. \quad (4)$$

The flux depends on the velocity of the objects, which we write as a function of the well-defined gravitational-wave frequency

$$v = \frac{G}{c^2}(\pi M f)^{\frac{1}{3}}. \quad (5)$$

The exact form of the flux and energy depends on the relativistic physics of the binary. With each additional term in the post-Newtonian expansion (around the ratio of the velocity to the speed of light) describing the energy and flux, different physics affects the gravitational-wave generation.

The flux of the system can be written schematically as

$$\mathcal{F} = \mathcal{F}(0pN) + \mathcal{F}(1pN) + \mathcal{F}(1.5pN) + \mathcal{F}(2pN) + \dots + (5pN) + \dots \quad (6)$$

To first order, gravitational waves depend on the chirp mass of the system, given by

$$\mathcal{M} = M\eta^{\frac{3}{5}}, \quad (7)$$

where  $M$  is the total mass and  $\eta = m_1 m_2 / M^2$  is the symmetric mass ratio. The lowest order, at 0pN, introduces the effect of the mass ratio. The third term introduces the leading order spin effect. The 2 pN term relates to the spin-spin of the binary [6]. Only at 5 pN order does the tidal deformation begin to affect the waveform. However, since the coefficients of the pN orders do not necessarily decrease monotonically, the 5pN term can still have a significant effect on the overall phase evolution of the waveform.

The energy balance equation allows us to derive the gravitational waveform as a function of time. The stationary phase approximation treats the phase as a constant, allowing us to look at the approximate energy or flux of the system at a given moment of the inspiral. Using this stationary phase approximation, this flux can be written directly in the frequency domain, a useful tool for parameter estimation.

If one of the objects is a neutron star, the gravity of its partner will cause tidal deformations in the star. However, the degree of the tidal deformation depends on the nuclear equation of state [7]. A stiff EOS implies that the force between the particles is quite strong, allowing it to maintain its shape as a less dense, larger star. A soft EOS implies that little force exists between the particles, so the matter is squeezed by gravity

into a smaller, denser star. As two neutron stars orbit each other until they collide, they emit a gravitational wave that is imprinted with information about the EOS through the tidal deformation of the stars. By analyzing these gravitational waves, we can learn about the nuclear EOS.

## 2. Status of Previous Research

Previous research has studied: (i) the amount of deformation (reflected in the quadrupole moment of the neutron stars) on the inspiral waveform given different models of tidal deformity; (ii) the signatures of a post-merger gravitational wave signal from a hypermassive neutron star or collapse to a black hole; and (iii) the ability of LIGO to measure the nuclear EOS from these waves.

Much of the literature focuses on extracting parameters on the inspiral phase of the gravitational wave where the frequency of the wave is in LIGO's most sensitive band: Flanagan et al. focused on information that could be extracted below a frequency of 400 Hz, finding that aLIGO should be able to constrain the tidal deformability of neutron stars to within  $2.0 \times 10^{37} g \times cm^2 \times s^2$  with 90% confidence for waves from symmetric binary neutron star systems with a total mass of  $2.8 M_{\odot}$  at a distance of 50 Mpc [8]. Hinderer et al. calculated the tidal deformability in the inspiral phase for several models of nuclear EOS and concluded that binaries at a distance of 100 Mpc could only constrain the nuclear EOS if it was particularly stiff [9]. Damour et al. found that the nuclear EOS can be constrained strongly with a loud binary neutron star gravitational-wave with a signal-to-noise ratio of 16 or more [10]. Wade et al. uses Bayesian parameter estimation to determine the measurability of the EOS with BNS signals. They also looked at how comparing the deformability and the chirp mass can narrow the possibilities for the neutron-star equation of state and the effect of biases and noise fluctuations on the accuracy of the measurements, finding that errors in the waveforms can bias the estimation of the tidal parameters [11]. Lackey et al. investigated ways to stack multiple BNS signals to measure the EOS. They found that about a years worth of detections should constrain the neutron-star EOS. In the low-mass range, the radius can be measured to within one kilometer and the deformability to within  $1 \times 10^{36} g \times cm^2 \times s^2$ , mainly constrained by the five loudest events [7]. Agathos et al. have studied the possibility for Advanced LIGO and Virgo to measure the nuclear EOS and included the effects of the spin of the neutron stars, of higher-order tidal effects, of the the quadrupole-monopole interaction and the cut-off frequency of the gravitational waves. They estimated the component masses of binary neutron star systems from gravitational waves simulated with distributions reflecting electromagnetic observations. The uncertainty about the mass distribution increases the number of binaries that need to be detected to distinguish between different types of EOS [12].

Alternatively, a few research groups have looked at extracting information from only the post-merger signal. Vines et al. analyzed the tidal higher-order effects and found that the changing quadrupole moment could increase the tidal effects by up to

20% in frequencies over 400 Hz [13]. In this work, Takami et al. performed a set of numerical simulations of the late inspiral, merger, and post-merger dynamics of binary neutron stars. They found a method of extracting the tidal deformability from BNS waves by comparing different analytical models and identifying two main features that consistently appeared in the waves: a high frequency peak associated with the formation of a supermassive neutron star and a low frequency peak associated with the merger process and the density of the stars. Using these parameters, tight constraints can be placed on possibilities for the neutron star EOS [14].

Little research has been done on extracting information on both the inspiral and the post-merger portions of the waveform. There is a significant amount of interesting physics in both the inspiral and the post-merger signal, despite the lower signal-to-noise ratio in the latter. During these portions of the waveforms, the stars will cause tidal disturbances in each other. The two stars collide, resulting in three possible remnants of the collision. One possibility is the formation of a quasi-stable supermassive neutron star. If the result is too dense, however, a black hole could form. This would occur when the total mass of the system that remains gravitationally bound is sufficiently large causing gravity to overcome the internal forces of the star, collapsing the neutron star matter into a black hole. The last possibility is a cross between these two: the collision could generate a large but unstable neutron star. The supermassive star could begin to form, but would then collapse into a black hole once the matter had settled into too dense of a state.

Each of these possibilities depend on the EOS of the neutron stars. Since soft equations of state tend to correspond with more dense neutron stars, neutron stars with soft equations of state are more likely to form a black hole upon collision. Conversely, stiff equations-of-state give rise to larger stars, which would feel tidal effects much earlier in the inspiral phase. If lots of matter is ejected from the binary system, the remaining mass is more likely to be small enough to form a quasi-stable remnant neutron star.

The resulting gravitational waves show significant alterations in the higher frequency band depending on the result of the collision, with each wave being distinct to the true EOS. Detecting such waves would help us constrain the possibilities for EOS of neutron stars. In Figure 1, we see the gravitational waves of two possible neutron star mergers of  $1.35 M_{\odot}$  [15]. The wave predicted from a softer equation of state is shown on the left, while the stiffer one is shown on the right. These waves exemplify both the effect the tidal deformability has on the resulting waveform and the variance between different predicted equation of states. The differences are distinct enough that sensitive ground-based detectors should be able to identify these different waves.

### **3. Approach**

Our goal is to determine LIGOs ability to measure the deformability of neutron stars from its effect on gravitational waves binary neutron star mergers. By analyzing multiple simulated events, we can explore our ability to constrain the nuclear equation-of-state.

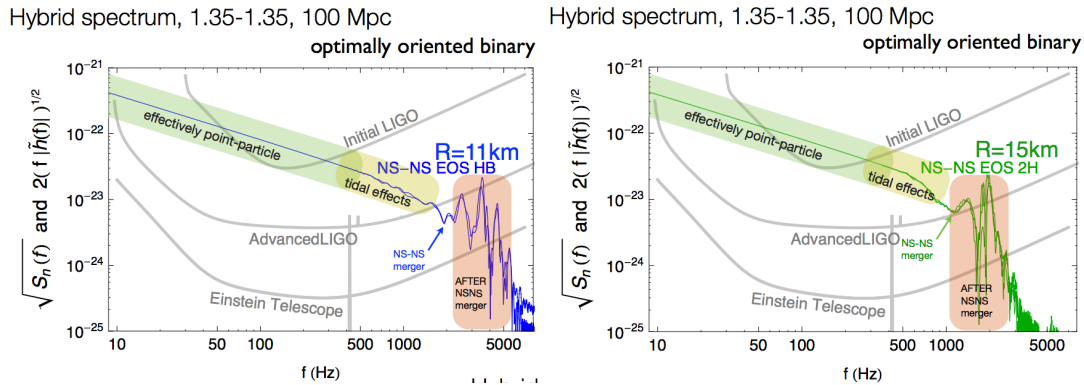


**Figure 1.** Gravitational waves of binary neutron star systems with  $1.35 M_{\odot}$  for each star compared to various noise spectra. The left graph is for a soft equation-of-state, while the right graph is for a hard equation-of-state.

As a first step, we derive the gravitational waveform from binary inspiral up to one-and-a-half post-Newtonian order. The calculation of the waveform to higher post-Newtonian orders is similar to that described above, albeit with more complicated algebra. At  $1.5\text{pN}$  order the flux is given by

$$\mathcal{F} = \frac{32}{5} \left(\frac{\mu}{M}\right)^2 v^{10} \left(1 + \left(-\frac{3}{4} - \frac{5\eta}{4}\right)v^2 + 4\pi v^3 + \mathcal{O}(v^4)\right), \quad (8)$$

and the energy is given by

$$\mathcal{E} = \mu - \mu v^2 \left[1 + \left(\frac{-3}{4} - \frac{\eta}{12}\right)v^2 + \mathcal{O}(v^4)\right]. \quad (9)$$

However, these equations treat the components of the binary as point particles. A gravitational wave from a binary neutron star system would have changes to  $\mathcal{F}$  and  $\mathcal{E}$  due to deformability of the stars in the binary. These changes are well-established and, using the inspiral portion of the wave, we can measure the tidal deformability and use the method Takami et al. created to generate the associated mergers and ringdowns of the binary system. We could next see whether this signal is found in the detector data. Thus, we will focus on analyzing inspiral waves with different tidal parameters. By comparing the extracted information to the input parameters of the simulated waves, we can test the reliability of this method.

The project will be successful if post-merger signals can be measured similarly to Takami et al. in a set of real LIGO data using Bayesian statistical analysis, the tidal deformability calculated using the inspiral accurately predicts the post-merger signature, and this combination of analyzing the inspiral and post-merger allows us to gain insight into the nuclear EOS.

#### 4. Preliminary Investigation

My project focuses on the post-merger portion of a binary neutron star waveform. This point corresponds to the part of inspiral where the tidal forces tear the star apart. This

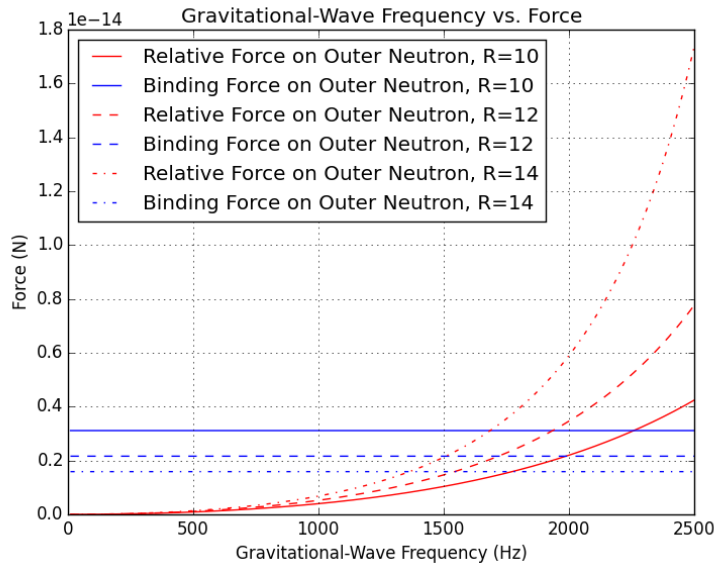


**Figure 2.** This plot shows the relative force and binding force as a function of gravitational-wave frequency. While the binding force (in blue) remains constant, the relative tidal forces (in red) increase as the binaries inspiral closer and faster, releasing gravitational waves at a higher frequency. The solid line represents a star system with a soft equation-of-state and by extension, stars with smaller radii, while the dashed line and dotted line correspond to progressively more stiff equations-of-state. The stars in the system would be ripped apart when the relative tidal force overcomes the related binding force.

occurs when the the relative tidal force on the edge of the star compared to that at the inside of the star overwhelms the binding force, pulling the star apart. To familiarize myself with the topic, we wrote preliminary code which calculated the force on individual neutrons in different parts of the star. This code calculated these forces for different neutron star radii, which correspond to different nuclear equations-of-state. The results from this code can be found in Figure 2. As can be seen from this plot, neutron stars with a stiff equations-of-state (and thus, larger radii) are torn apart more quickly than those with soft equations-of-state (and smaller radii). The largest star system would be torn apart at 1.3 kHz, when the relative force overwhelmed the binding force, while the smallest star is torn apart at 2.25 kHz. This simple argument outlines the effects of two nuclear equations-of-state qualitatively.

## 5. Parameter Estimation

We began our investigation with an introduction to parameter estimation using a set of data containing injections which had been analyzed by the parameter estimation pipeline `lal inference` [16, 17]. This program works by comparing a parameterized model to the detected gravitational wave. In Fig. 3, we find an example of the type of

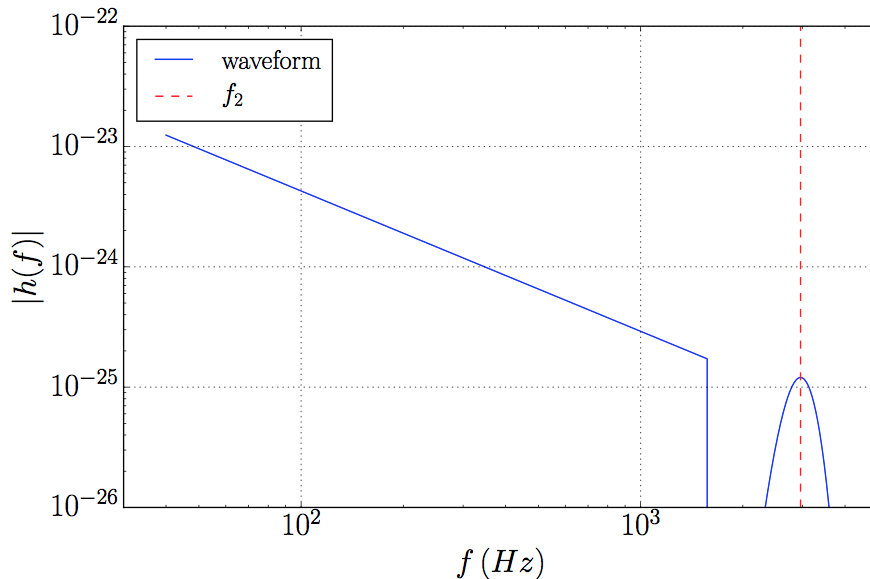


**Figure 3.** This figure describes the type of toy model to which a detected gravitational wave is compared. This plot shows the strain of the model as a function of the frequency. Like the simulated gravitational waves in Fig. 1, we see a decrease in strain representing the inspiral phase of the binary and a peak representing the post-merger signal.

model to which the detected gravitational wave is compared. This toy model represents a simplified version of a binary neutron-star gravitational wave. Like real numerical simulations show, the toy model contains a low-frequency inspiral phase followed by a post-merger peak, located at a fixed frequency. The numerical simulations include many subtle differences, including a decrease in power at the end of the low-frequency phase due to tidal deformation and variability on the peak frequency, height and width. Different models could lead to varying outcomes in `lalinference`'s performance.

In this investigation, we compare analyses using three different models. The first is reflects previous investigations which looked only at the inspiral phase of the model and contains no post-merger peak. The second analysis used a model that contained a post-merger peak whose height was set to 8 times the strain just before merger. Since the deformability of the neutron star is not known and this parameter dictates the post-merger signal, the height, position and width of this peak is not known *a priori*. However, this peak frequency can be parameterized using *Love numbers* and assuming a model for the nuclear equation-of-state. These parameters describe the deformation of non-rigid objects in different directions with respect to the mass causing tides. The second Love number,  $k_2$ , can be used to relate  $\kappa_2^T$ , a quantity that determines the dynamics of a merger, to the deformability of neutron stars,  $\lambda$ :

$$\kappa_2^T = 2 \left( \frac{q^4}{(1+q)^5} \frac{k_2^A}{C_A^5} + \frac{q}{(1+q)^5} \frac{k_2^B}{C_B^5} \right). \quad (10)$$

where  $q$  is the mass ratio of the neutron stars. Since the deformability  $\lambda$  directly depends



on this Love number, we can directly relate  $\kappa_2^T$  to the deformability given by various proposed nuclear equation-of-state models:

$$\lambda(m) = \frac{2}{3}k_2(m)R^5(m), \quad (11)$$

where  $R$  is the radius of the star given the assumed nuclear equation-of-state.  $\kappa_2^T$  directly influences the location of the peak frequency in the post-merger portion of the waveform [18]. However, we do not know which model is correct when analyzing astrophysical signals. For this reason, our third analysis uses a variable height on the post-merger.

The deformability of a neutron star is represented by  $\lambda$ . The deformability can be expanded using a Taylor series:

$$\lambda(m) \simeq c_0 + c_1 \left( \frac{m - m_0}{M_\odot} \right) + \frac{1}{2}c_2 \left( \frac{m - m_0}{M_\odot} \right)^2, \quad (12)$$

where  $m$  is the mass of the neutron star and  $m_0$  is a reference mass [?]. The first-order approximation of the deformability is  $c_0$ . This parameter is most easily estimated by aLIGO and Virgo, since it has the largest correction to the waveform. Using the parameters  $c_0$  and  $\kappa_2^T$ , we refine the model in Fig. 3 for our analyses.

The parameter estimation pipeline `lalinferenc` uses the given toy model and compares it to the data containing the detected gravitational wave. The pipeline then uses a Markov Chain Monte Carlo (MCMC) to step through the parameter space and uses Bayesian inference to compute the likelihood of the data as a function of the parameter values. In particular, we know that the probability of a parameter  $\theta$  being the correct value given the data  $x$  is proportional to the probability of getting the data given the parameter times the probability of the parameter being the correct value:

$$p(\theta|x) \propto p(x|\theta) \times p(\theta). \quad (13)$$

With each successive detected gravitational wave, we will be able to extract more information about the parameter. The probability that  $\theta$  is the correct value given both the first detection  $x$  and the second detection  $y$  is

$$p(\theta|x, y) = p(x, y|\theta) \times p(\theta). \quad (14)$$

This can be rewritten as

$$p(\theta|x, y) = p(y|\theta, x) \times p(\theta|x). \quad (15)$$

However, since gravitational waves are uncorrelated, the probability of  $y$  cannot depend on the  $x$ , meaning that using 13 we can write this function as

$$p(\theta|x, y) = p(y|\theta) \times p(x|\theta) \times p(\theta). \quad (16)$$

Therefore, in order to calculate the probability of find the parameter to be  $\theta$  given two data sets, we need only to multiply the probabilities for the individual detections together.

To find the probability of the parameter given many detections, we need only multiply the probabilities of each detection together in the same way as above:

$$p(\theta|x_i) = \left[ \prod_i p(x_i|\theta) \right] p(\theta). \quad (17)$$

Thus, using the output of `lalinference`, we can create probability density functions for the parameters from each gravitational wave detection then simply multiply the functions together to estimate the probability function for the parameter given all the collected data. For our analysis, we focus in particular on `lalinference`'s estimation of the first-order of this expansion,  $c_0$ . Comparing estimations for many gravitational-wave signals can strongly constrain the deformability parameter of neutron stars.

To test our pipeline, we analyze several types of binary neutron-star simulations, which we add to LIGO data, called *injections*. These simulated signals represent the type of detections that would give us more information about the nuclear EOS. This method assumes the gravitational waves share a common deformability parameter. Combining information from each successive injection allows us to construct a new probability density function for the cumulative set of injections. This allows us to strongly constrain the deformability of the neutron-star equation of state. This iteration method is demonstrated in Fig. 4.

From these probability density functions, we are able to constrain the neutron star deformability parameter  $c_0$  in a 95% confidence interval. The successive detections allow us to shrink the confidence interval, allowing for a more precise measurement of the deformability parameter. By looking at the confidence intervals as a function of detections, we can see how the many injections are required to constrain the possible deformabilities.

Fig. 5 demonstrates how the confidence interval shrinks with new information from more injections. These plots also demonstrate how the confidence intervals for different equation-of-state models shrink differently and focus on their corresponding deformabilities. To properly compare the performance of these analyses we compare the widths of the confidence intervals in Fig. 6. Ideally, a high-performing pipeline would produce small confidence intervals, i.e. would strongly constrain the parameter. We see from this figure that while the analyses do perform similarly, the analysis using a variable-height post-merger peak tends to constrain the deformability more weakly than the other analyses, while the analysis using a fixed-height post-merger peak performs better. This implies that introducing the uncertainty from the peak's varying height does not aid in constraining the deformability, as one would expect, since the model does not reveal any new information of the deformability on the peak height. In reality and in a more realistic model, the peak height would depend on the EOS through the deformability, so that learning about the height of the post-merger signal would allow us to more easily constrain the deformability of the neutron star.

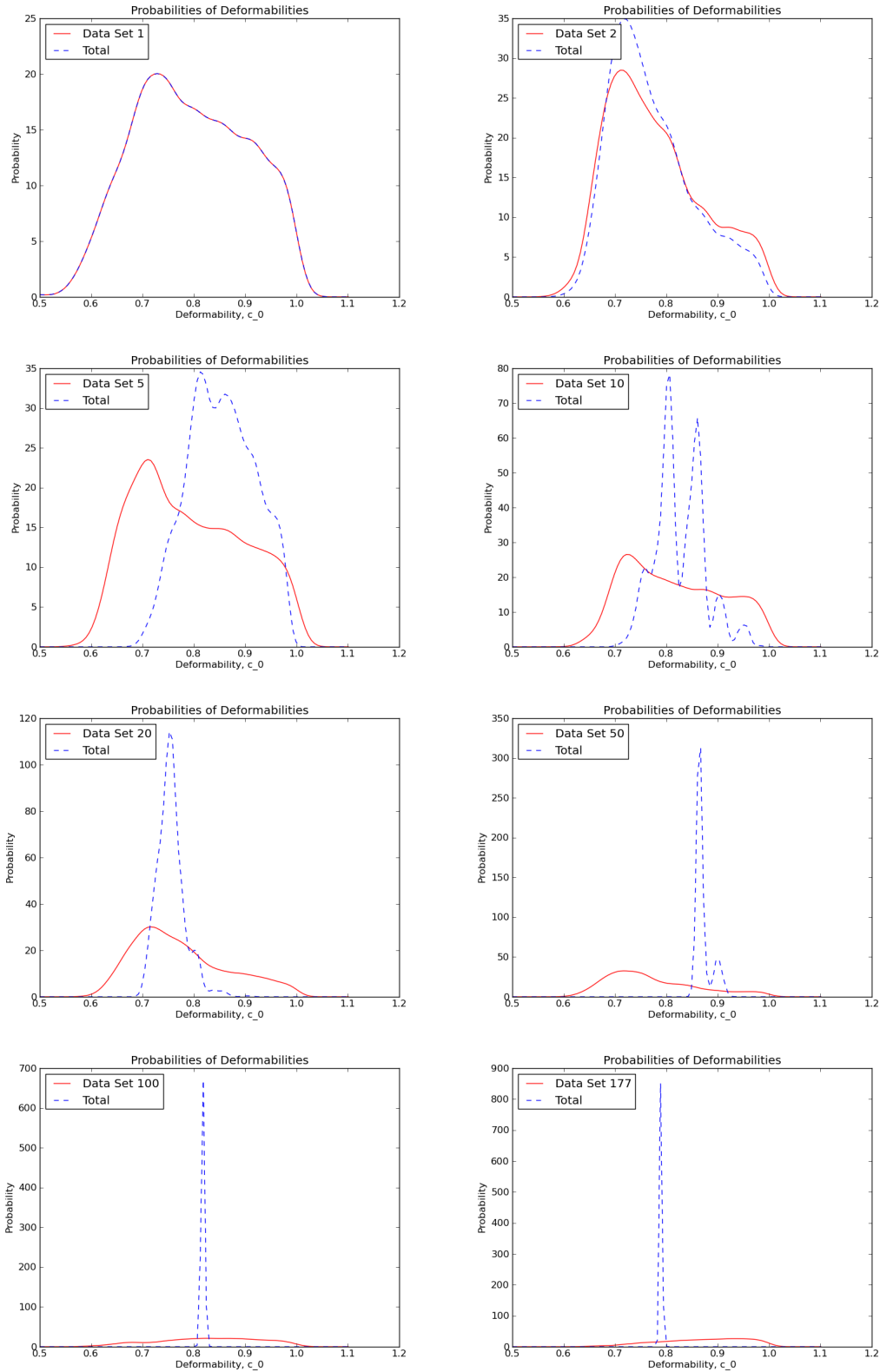


**Figure 4.** These plots show the probability function for deformabilities of multiple injections made using the MS1 model. The solid, red line represents the probability density function for the newest injection’s data; the dashed line represents the data; the probability density function from all injected signals in the set. Representative plots are shown for detections 1, 2, 5, 10, 20, 50, 100 and (the final) 177.

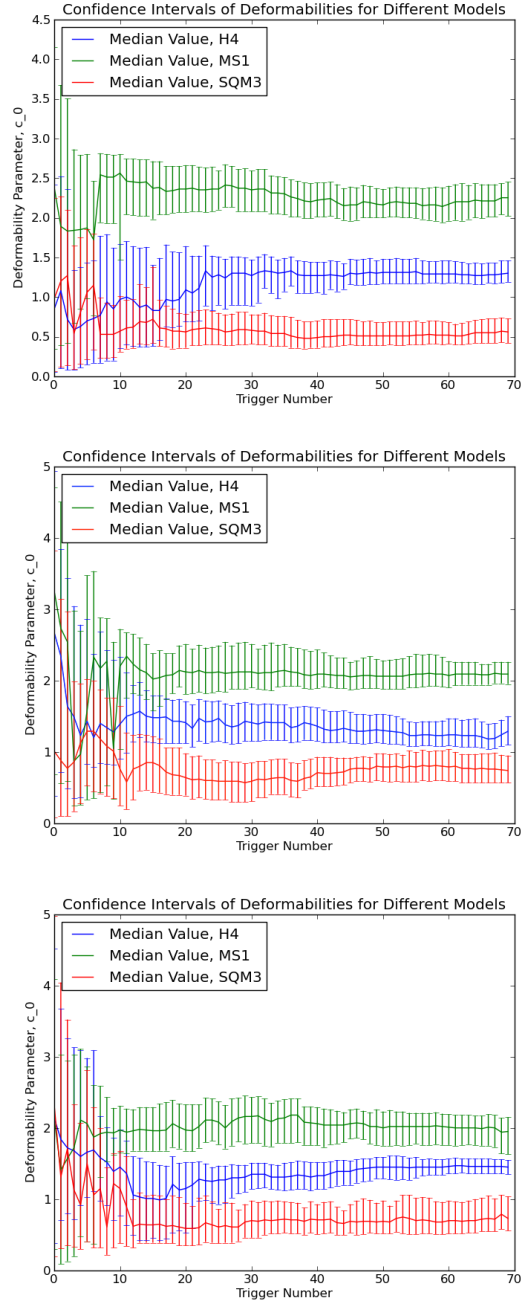


**Figure 5.** These plots present the confidence intervals of three types of models of injections. The x-axis represents the number of detections analyzed, while the y-axis represents the estimate of the deformability parameter and its 96% confidence interval. The three models used here are H4 (blue), MS1 (green) and SQM3 (red). The top plot was created for the analysis using no post-merger signal, the middle for the analysis using a fixed-peak post-merger signal and the bottom for the analysis using a variable height post-merger signal. With each successive injection, the confidence interval converges on a smaller possibility for deformability. Since the ordering in which our simulated signals are analyzed is arbitrary, we analyze 1,000 different orders for each type of signal then average the confidence interval for each.

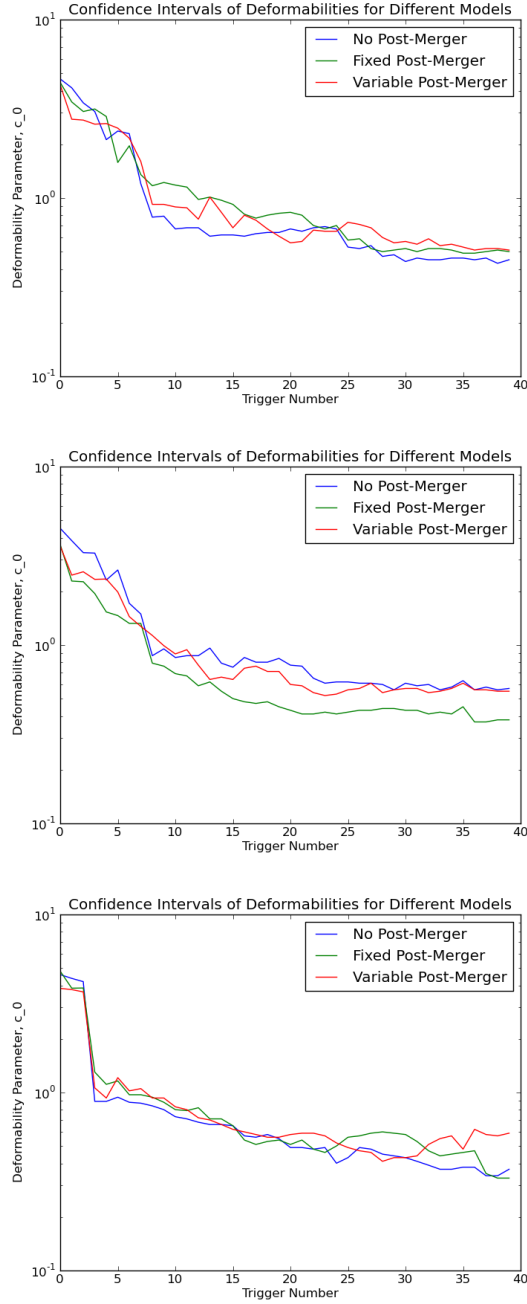


**Figure 6.** These three plots describe the widths of the deformability confidence intervals as a function of detections. Each line describes a different model to which the parameter estimation pipeline `lal inference` compared the simulated signal; the model with no post-merger peak is in blue, the model with a fixed-height post-merger peak is in green and the model with a varying-height post-merger peak is in red. The top plot were the analyses for simulated signals generated with the H4 model for the nuclear EOS, the middle plot with the MS1 model, and the bottom plot with the SQM3 model. As before, the width of the confidence intervals have been averaged over 1,000 possible permutations of detections since the order of our detections are arbitrary.

## 6. Conclusions & Future Work

From our investigation, we conclude that using post-merger signals when analyzing binary neutron-star signals can help constrain the deformability of neutron stars. However, introducing uncertainties about the post-merger signal can detract from the amount of information extracted from the signals. For this reason, further research should aim to refine the model used to analyze the signals. In particular, identifying the effects of the nuclear EOS on the post-merger signals can aid in the pipeline's ability to constrain the nuclear EOS. Using this information would allow us to create a more accurate model to compare to signals in order to more strongly identify the neutron-star deformability without introducing uncertainties to weaken our analysis.

## References

- [1] Abbott B *et al.* (LIGO Scientific) 2009 *Rept.Prog.Phys.* **72** 076901 (*Preprint* 0711.3041)
- [2] Accadia T *et al.* (VIRGO) 2012 *JINST* **7** P03012
- [3] Akutsu T (KAGRA) 2015 *J.Phys.Conf.Ser.* **610** 012016
- [4] Thorne K 1987 *Gravitational Radiation* (Cambridge University Press)
- [5] Ozel F, Psaltis D, Narayan R and Villarreal A S 2012 *Astrophys.J.* **757** 55 (*Preprint* 1201.1006)
- [6] Aasi J *et al.* (LIGO Scientific, VIRGO) 2013 (*Preprint* 1304.0670)
- [7] Lackey B D and Wade L 2015 *Phys.Rev.* **D91** 043002 (*Preprint* 1410.8866)
- [8] Flanagan E E and Hinderer T 2008 *Phys. Rev. D* **77**(2) 021502 URL <http://link.aps.org/doi/10.1103/PhysRevD.77.021502>
- [9] Hinderer T, Lackey B D, Lang R N and Read J S 2010 *Phys.Rev.* **D81** 123016 (*Preprint* 0911.3535)
- [10] Damour T, Nagar A and Villain L 2012 *Phys. Rev. D* **85**(12) 123007 URL <http://link.aps.org/doi/10.1103/PhysRevD.85.123007>
- [11] Wade L, Creighton J D, Ochsner E, Lackey B D, Farr B F *et al.* 2014 *Phys.Rev.* **D89** 103012 (*Preprint* 1402.5156)
- [12] Agathos M, Meidam J, Del Pozzo W, Li T G F, Tompitak M *et al.* 2015 (*Preprint* 1503.05405)
- [13] Vines J, Flanagan E E and Hinderer T 2011 *Phys.Rev.* **D83** 084051 (*Preprint* 1101.1673)
- [14] Takami K, Rezzolla L and Baiotti L 2015 *Phys.Rev.* **D91** 064001 (*Preprint* 1412.3240)
- [15] Read J S, Baiotti L, Creighton J D E, Friedman J L, Giacomazzo B *et al.* 2013 *Phys.Rev.* **D88** 044042 (*Preprint* 1306.4065)
- [16] Li T Private communication
- [17] Veitch J *et al.* 2015 *Phys. Rev. D* **91**(4) 042003 URL <http://link.aps.org/doi/10.1103/PhysRevD.91.042003>
- [18] Bernuzzi S, Dietrich T and Nagar A 2015 *Phys. Rev. Lett.* **115**(9) 091101 URL <http://link.aps.org/doi/10.1103/PhysRevLett.115.091101>